

Borole Derivatives. 20.¹ Three-Center Fe–H–B Bonding in (Borole)(cyclopentadienyl)hydridoiron Derivatives

Gerhard E. Herberich,* Tobias Carstensen, Dieter P. J. Köffer, and Norbert Klaff

*Institut für Anorganische Chemie, Technische Hochschule Aachen,
Professor-Pirlet-Strasse 1, D-52056 Aachen, Germany*

Roland Boese

*Institut für Anorganische Chemie, Universität-GH Essen,
Universitätsstrasse 3-5, D-45117 Essen 1, Germany*

Isabella Hyla-Kryspin and Rolf Gleiter*

*Institut für Organische Chemie der Universität Heidelberg,
Im Neuenheimer Feld 270, D-69120 Heidelberg, Germany*

Martin Stephan

*Institut für Anorganische Chemie der Universität Heidelberg,
Im Neuenheimer Feld 270, D-69120 Heidelberg, Germany*

Helmut Meth and Ulrich Zenneck*

*Institut für Anorganische Chemie der Universität Erlangen-Nürnberg,
Egerlandstrasse 1, D-91058 Erlangen, Germany*

Received July 26, 1993*

(Borole)tricarbonyliron complexes $\text{Fe}(\text{CO})_3(3,4\text{-R}^1_2\text{C}_4\text{H}_2\text{BPh})$ (**3a**, $\text{R}^1 = \text{H}$; **3b**, $\text{R}^1 = \text{Me}$) react with cyclopentadiene under irradiation to give the hydrides $\text{CpFeH}(3,4\text{-R}^1_2\text{C}_4\text{H}_2\text{BPh})$ (**1a**, **b**). Deprotonation by NaH in THF produces the borataferrocene anions $[\text{CpFe}(3,4\text{-R}^1_2\text{C}_4\text{H}_2\text{BPh})]^-$ (**5a**, **5b**). These can be alkylated in the 2-/5-position by alkyl iodides in the presence of NaH to give 2,5-dialkyl hydride derivatives: e.g. $\text{CpFeH}(2,5\text{-R}^2_2\text{C}_4\text{H}_2\text{BPh})$ (**1c**, $\text{R}^2 = \text{Me}$; **1g**, $\text{R}^2 = \text{CH}_2=\text{CH}(\text{CH}_2)_4$; **1h**, $\text{R}^2 = (\text{CH}_2)_2\text{CHCH}_2$). The structures of $\text{CpFeH}(2,3,4,5\text{-Me}_4\text{C}_4\text{BPh})$ (**1d**; $\text{Fe-B} = 215.1(4)$ pm, $\text{Fe-H} = 147(3)$ pm, $\text{B-H} = 151(3)$ pm) and $(\text{C}_5\text{H}_4\text{Me})\text{FeH}(2,5\text{-Me}_2\text{C}_4\text{H}_2\text{BPh})$ (**1f**; $\text{Fe-B} = 215.5(2)$ pm, $\text{Fe-H} = 147.5(23)$ pm, $\text{B-H} = 146.1(26)$ pm) as determined by low-temperature X-ray diffraction show the presence of an Fe–H–B three-center bond with a weak B–H interaction. In solution **1a** establishes a mobile equilibrium between the ground state **1a-G** with Fe–H–B three-center bonding and the agostic isomer **1a-A** with Fe–H–C-2($\text{C}_4\text{H}_4\text{B}$) three-center bonding with an estimated $\Delta G = 1.4$ kcal/mol. The hydridic proton and the 2-/5-protons of the borole ring undergo fast intramolecular exchange ($T_c = 333$ K at 80 MHz and $\Delta G^\ddagger_{333} = 17.0 \pm 0.7$ kcal/mol for **1a**). A merry-go-round of the three H atoms involved with one hydrogen crossing the exo face of the borole ligand is proposed as an exchange mechanism. The bonding in $\text{CpFeH}(\text{C}_4\text{H}_4\text{BH})$ is analyzed by means of extended Hückel calculations, which confirm the Fe–H–B three-center bonding. Exploratory extended Hückel calculations also support the existence of agostic isomers as well as the proposed exchange mechanism. Cyclic voltammetry revealed the existence of the 17e complex $\text{CpFe}(\text{C}_4\text{H}_4\text{BPh})$ (**5a**), which is characterized by its EPR and paramagnetic ^1H NMR spectra. **1a** reacts with CNBu^t to give the boracyclopentenyl complex $\text{CpFe}(\text{CNBu}^t)(\text{C}_4\text{H}_5\text{BPh})$ (**9a**) and, probably via the intermediate $\text{Fe}(\text{CNBu}^t)(\text{C}_4\text{H}_4\text{BPh})(\text{C}_5\text{H}_6)$ (**10**), the borole complex $\text{Fe}(\text{CNBu}^t)_3(\text{C}_4\text{H}_4\text{BPh})$ (**11a**) and 1 equiv of cyclopentadiene. Labeling experiments show that the shift of the hydridic hydrogen to the borole and Cp ligands, respectively, is an intramolecular process. **1c** reacts analogously.

Introduction

A great number of metal borole complexes, including triple-decker compounds, have been described in recent years.^{1,2} While the chemistry of the borole ligand is well established, free 1H-boroles are highly reactive four- π -electron systems^{3–6} and only a few sterically protected

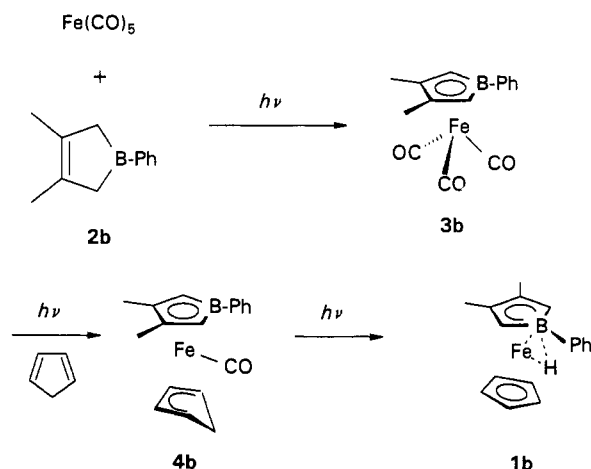
derivatives have been isolated to date.^{5,6} Qualitative MO considerations show that the borole system possesses a diene-like HOMO and a low-lying LUMO. These properties favor transition-metal complexes with strong metal-to-ligand back-bonding. Anionic complexes, e.g. $[\text{RhL}_2]^-$,⁷

(2) (a) Reference 1 and references quoted therein. (b) Herberich, G. E.; Köffer, D. P. J.; Peters, K. M. *Chem. Ber.* 1991, 124, 1947 and references quoted therein. (c) Hong, F.-E.; Fehlner, T. P.; Rheingold, A. L. *Organometallics* 1991, 10, 1213. (d) Sebald, A.; Wrackmeyer, B. *J. Organomet. Chem.* 1986, 304, 271.

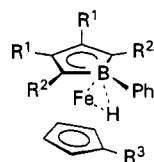
(3) Herberich, G. E.; Ohst, H. *Chem. Ber.* 1985, 118, 4303.

* Abstract published in *Advance ACS Abstracts*, January 1, 1994.
(1) Part 19: Herberich, G. E.; Carstensen, T.; Englert, U. *Chem. Ber.* 1992, 125, 2351.

Scheme 1



$[\text{CoL}_2]^-$,⁸ $[\text{CpFeL}]^-$,⁹ $[\text{LRe}(\text{CO})_3]^-$,¹⁰ $[\text{LFeH}(\text{CO})_2]^-$,¹¹ and $[\text{LCo}(\text{CO})_2]^-$ ($\text{L} = \text{C}_4\text{H}_4\text{BPh}$), show only poor basicity (the Co and Rh systems with two borole ligands exist in neutral aqueous solution) owing to delocalization of the negative charge by back-bonding. As far as first-row transition-metal complexes are concerned, the corresponding hydrides often possess unusual nonclassical properties. In this paper we describe the synthesis and reactivity of the (borole)(cyclopentadienyl)iron hydrides **1** and of the corresponding anions. The structural problems associated with the hydrides **1**, both in the crystalline state and in solution, are addressed in detail.



- 1a:** $\text{R}^1, \text{R}^2, \text{R}^3 = \text{H}^9$
b: $\text{R}^1 = \text{Me}; \text{R}^2, \text{R}^3 = \text{H}$
c: $\text{R}^1 = \text{H}; \text{R}^2 = \text{Me}; \text{R}^3 = \text{H}$
d: $\text{R}^1, \text{R}^2 = \text{Me}; \text{R}^3 = \text{H}$
e: $\text{R}^1, \text{R}^2 = \text{H}; \text{R}^3 = \text{Me}$
f: $\text{R}^1 = \text{H}; \text{R}^2, \text{R}^3 = \text{Me}$
g: $\text{R}^1 = \text{H}; \text{R}^2 = \text{CH}_2=\text{CH}(\text{CH}_2)_4; \text{R}^3 = \text{H}$
h: $\text{R}^1 = \text{H}; \text{R}^2 = (\text{CH}_2)_2\text{CHCH}_2; \text{R}^3 = \text{H}$

Results

Syntheses. The synthesis of **1a** has been reported previously.⁹ The derivatives **1b,e** were made by the same route, which is summarized in Scheme 1. For the preparation of **1b** the 3,4-dimethylborolene species **2b**¹² is treated with $\text{Fe}(\text{CO})_5$ under irradiation. The ensuing

(4) Fagan, P. J.; Burns, E. G.; Calabrese, J. C. *J. Am. Chem. Soc.* **1988**, *110*, 2979.

(5) (a) Eisch, J. J.; Galle, J. E.; Kozima, S. *J. Am. Chem. Soc.* **1986**, *108*, 379. (b) Herberich, G. E.; Buller, B.; Hessner, B.; Oschmann, W. *J. Organomet. Chem.* **1980**, *195*, 253. (c) Eisch, J. J.; Galle, J. E.; Shafii, B.; Rheingold, A. L. *Organometallics* **1990**, *9*, 2342.

(6) Sebald, A.; Wrackmeyer, B. *J. Organomet. Chem.* **1986**, *307*, 157.

(7) Herberich, G. E.; Büschges, U.; Hessner, B.; Lütke, H. *J. Organomet. Chem.* **1986**, *312*, 13.

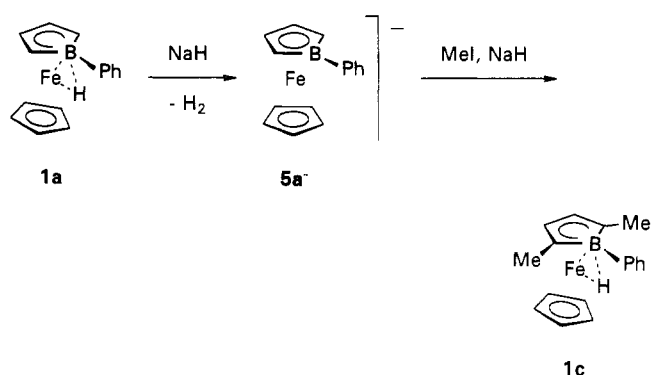
(8) Herberich, G. E.; Hessner, B.; Saive, R. *J. Organomet. Chem.* **1987**, *319*, 9.

(9) Herberich, G. E.; Hessner, B.; Köffer, D. P. *J. Organomet. Chem.* **1989**, *362*, 243.

(10) Herberich, G. E.; Dunne, B. J.; Hessner, B. *Angew. Chem., Int. Ed. Engl.* **1989**, *28*, 737.

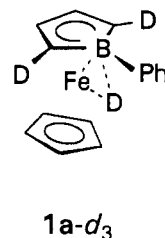
(11) Herberich, G. E.; Carstensen, T.; Klaff, N.; Neuschütz, M. *Chem. Ber.* **1992**, *125*, 1801.

Scheme 2



dehydrogenative complex formation¹³ affords the borole complex **3b**. In the presence of cyclopentadiene this complex **3b** readily undergoes photochemical substitution to produce the monocarbonyl diene derivative **4b**, which, on prolonged irradiation, forms the hydride **1b**.

The hydrides **1a,b,e**, which do not carry substituents at the 2-/5-position of the borole ring, are very air-sensitive red solids with a characteristic smell. Pure samples could be stored under inert gas for several months. However, traces of impurities can cause spontaneous decomposition even at -30°C . Contact with excess D_2O effects instantaneous H/D exchange of the hydrogen atoms at the iron and, surprisingly, at the 2-/5-position of the borole ligand; this process affords, e.g., **1a-d₃**.



The hydridic hydrogen is readily removed by NaH, yielding sodium salts of borataferrocene anions **5a⁻**, **5b⁻**, and **5e⁻**. **5a⁻** has previously been characterized as the $[\text{Li}(\text{TMEDA})]^+$ salt.⁹ The anions **5a⁻**, **5b⁻**, and **5e⁻** react with methyl iodide in the presence of excess NaH to afford the 2,5-dimethylated hydride complexes **1c,d,f** (Scheme 2).

Monitoring the methylation by NMR spectroscopy shows that the monomethyl derivatives cannot be made selectively because of proton exchange between the various anionic and hydridic species in the reaction mixture. This exchange is fast even at -80°C . Radical clock reagents¹⁴ such as 1-iodo-5-hexene and (iodomethyl)cyclopropane produce the unrearranged products **1g,h** exclusively. This observation suggests that the alkylation proceeds via a straightforward $\text{S}_{\text{N}}2$ mechanism. Once the 2-/5-positions are alkylated, further alkylation is blocked.

(12) (a) Söhnen, D. Dissertation, RWTH Aachen, 1984. (b) Herberich, G. E.; Boveleth, W.; Hessner, B.; Hostalek, M.; Köffer, D. P. J.; Ohst, H.; Söhnen, D. *Chem. Ber.* **1986**, *119*, 420.

(13) Herberich, G. E.; Boveleth, W.; Hessner, B.; Köffer, D. P. J.; Negele, M.; Saive, R. *J. Organomet. Chem.* **1986**, *308*, 153.

(14) (a) Newcomb, M.; Curran, D. P. *Acc. Chem. Res.* **1988**, *21*, 206. (b) Newcomb, M.; Glenn, A. G. *J. Am. Chem. Soc.* **1989**, *111*, 275. (c) Bowry, V. W.; Luszyk, J.; Ingold, K. U. *J. Am. Chem. Soc.* **1991**, *113*, 5687. (d) Organometallic radicals such as CoCp_2 and $\text{CpFe}(\text{C}_6\text{Me}_6)$ undergo extremely fast addition reactions with aliphatic radicals: Herberich, G. E.; Carstensen, T.; Klein, W.; Schmidt, M. U. *Organometallics* **1993**, *12*, 1439.

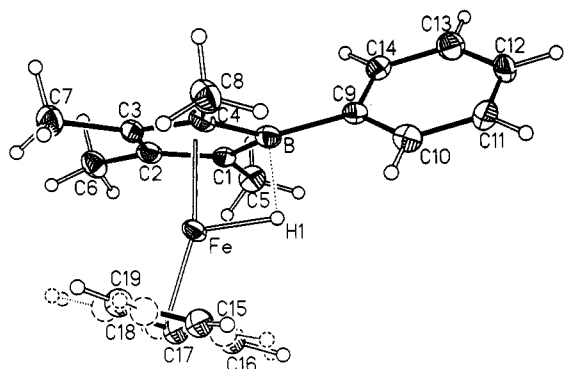


Figure 1. Presentation of the molecular structure (50% ellipsoids) of CpFeH(C₄Me₄BPh) (1d).

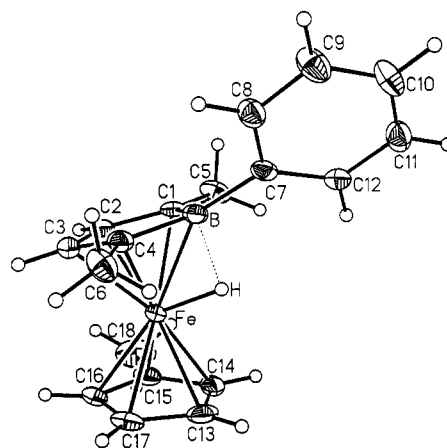


Figure 2. Presentation of the molecular structure (50% ellipsoids) of (C₅H₄Me)FeH(2,5-Me₂C₄H₂BPh) (1f).

Table 1. Atomic Coordinates of Non-Hydrogen Atoms and of the Hydridic Hydrogen Atom for 1d

atom	x	y	z	U _{eq}
Fe	0.6886(1)	0.6650(1)	0.0499(1)	19(1) ^a
H	0.6431(12)	0.6818(12)	-0.0180(42)	36(10) ^a
B	0.6287(1)	0.6318(1)	-0.0673(5)	21(1) ^a
C1	0.6768(1)	0.6252(1)	-0.1609(4)	19(1) ^a
C2	0.7097(1)	0.06020(1)	-0.0577(5)	20(1) ^a
C3	0.6886(1)	0.5922(1)	0.0976(4)	19(1) ^a
C4	0.06407(1)	0.06094(1)	0.1101(4)	19(1) ^a
C5	0.6894(1)	0.6418(1)	-0.3283(4)	27(1) ^a
C6	0.7595(1)	0.5871(1)	-0.1045(5)	26(1) ^a
C7	0.7140(1)	0.5682(1)	0.2345(5)	27(1) ^a
C8	0.6101(1)	0.6057(1)	0.2495(4)	29(1) ^a
C9	0.5773	0.6434	-0.1435	20(1) ^{a,b}
C10	0.5459(1)	0.6755(1)	-0.0705(2)	27(1) ^{a,b}
C11	0.5015	0.6844	-0.1407	32(1) ^{a,b}
C12	0.4886	0.6613	-0.2839	34(1) ^{a,b}
C13	0.5200	0.6293	-0.3569	33(1) ^{a,b}
C14	0.5643	0.6203	-0.2866	24(1) ^{a,b}
C15	0.6870(2)	0.7198(2)	0.2149(6)	22(1) ^{b,c}
C16	0.6979	0.7371	0.0573	22(1) ^{b,c}
C17	0.7408	0.7149	0.0053	22(1) ^{b,c}
C18	0.7564	0.6840	0.1308	22(1) ^{b,c}
C19	0.7232	0.6870	0.2604	22(1) ^{b,c}
C15a	0.6840(2)	0.7309(2)	0.1595(6)	22(1) ^{b,c}
C16a	0.7086	0.7358	0.0098	22(1) ^{b,c}
C17a	0.7498	0.7065	0.0159	22(1) ^{b,c}
C18a	0.7508	0.6836	0.1694	22(1) ^{b,c}
C19a	0.7101	0.6987	0.2581	22(1) ^{b,c}

^a Equivalent isotropic U_{eq}, defined as one-third of the trace of the orthogonalized U_{ij} tensor; in 10⁻¹ pm². ^b Atoms calculated as rigid groups have a standard deviation for the first atom only. ^c Disordered Cp ligands with a population of 1/2 each.

The 2,5-dialkylated complexes 1c,d,f form air-stable red crystals and are not air-sensitive, even in solution. In contrast to the unmethylated hydrides, they do not undergo H/D exchange with D₂O. With NaH no reaction takes place. Deprotonation of the sterically hindered tetramethyl complex 1d can be effected by LiBu in THF, while the 2,5-dimethyl complex 1c suffered reductive decomposition under these reaction conditions.

Crystal Structures of 1d and 1f. All attempts to grow crystals of 1a suitable for X-ray diffraction work were unsuccessful. However, the chemically robust derivatives 1d,f readily gave good crystals which allowed the determination of their structures at low temperature (1d, Figure 1, Tables 1 and 2; 1f, Figure 2, Tables 3 and 4). In the case of 1d rotational disorder of the cyclopentadienyl ring was encountered in spite of the low temperature of the measurement.

The molecules of 1d,f show a bent-sandwich structure with bending angles¹⁵ of 165.2 and 164.3°, respectively.

Table 2. Selected Bond Distances and Bond Angles for 1d

(a) Bond Distances (pm)			
Metal-Ligand and Borole			
Fe-B	215.1(4)	Fe-C1	209.3(3)
Fe-H	147(3)	Fe-C2	206.7(3)
B-H	151(3)	Fe-C3	208.1(3)
		Fe-C4	210.3(3)
B-C1	156.5(5)	B-C9	160.8(4)
C1-C2	141.4(5)	C1-C5	149.9(5)
C2-C3	143.7(5)	C2-C6	150.8(5)
C3-C4	142.7(4)	C3-C7	149.6(5)
B-C4	156.2(5)	C4-C8	149.9(5)
Cp Ring C15...C19a			
Fe-C _{min}	203.9(5)	Fe-C _{av}	206.8
Fe-C _{max}	209.4(5)		
(b) Bond Angles (deg)			
Fe-H-B	92(2)	B-C1-C2	108.7(3)
C1-B-C4	101.8(3)	C1-C2-C3	110.7(3)
C1-B-C9	127.3(3)	C2-C3-C4	110.0(3)
C4-B-C9	128.5(3)	C3-C4-B	108.7(3)

Table 3. Coordinates of Non-Hydrogen Atoms and of the Hydridic Hydrogen Atom for 1f

atom	x	y	z	U _{eq} ^a
Fe	0.5989(1)	0.2173(1)	0.8376(1)	16(1)
H	0.4962(20)	0.3161(30)	0.8041(15)	35(6)
B	0.5606(1)	0.4356(2)	0.7655(1)	19(1)
C1	0.6573(2)	0.4528(2)	0.8518(1)	20(1)
C2	0.7479(2)	0.3878(2)	0.8453(1)	21(1)
C3	0.7218(2)	0.2606(2)	0.7652(1)	22(1)
C4	0.6129(2)	0.3054(2)	0.7151(1)	21(1)
C5	0.6578(2)	0.5536(2)	0.9305(1)	29(1)
C6	0.5598(2)	0.2265(2)	0.6308(1)	29(1)
C7	0.4654(2)	0.5641(2)	0.7277(1)	19(1)
C8	0.4670(2)	0.6333(2)	0.6471(1)	25(1)
C9	0.3915(2)	0.7533(3)	0.6132(1)	33(1)
C10	0.3099(2)	0.8074(3)	0.6580(1)	32(1)
C11	0.3057(2)	0.7419(3)	0.7376(1)	28(1)
C12	0.3827(2)	0.6224(2)	0.7717(1)	22(1)
C13	0.4726(2)	0.0607(2)	0.8561(1)	30(1)
C14	0.5253(2)	0.1349(2)	0.9359(1)	28(1)
C15	0.6448(2)	0.0963(2)	0.9539(1)	25(1)
C16	0.6644(2)	0.0002(2)	0.8848(1)	25(1)
C17	0.5575(2)	-0.0233(2)	0.8248(1)	29(1)
C18	0.7331(2)	0.1416(3)	1.0327(2)	45(1)

^a Equivalent isotropic U_{eq}, defined as one-third of the trace of the orthogonalized U_{ij} tensor; in 10⁻¹ pm².

Both structures deviate very little from lateral symmetry, except for the rotational orientation of the phenyl group.

(15) The bending angle is the angle spanned by the perpendiculars of the two rings.

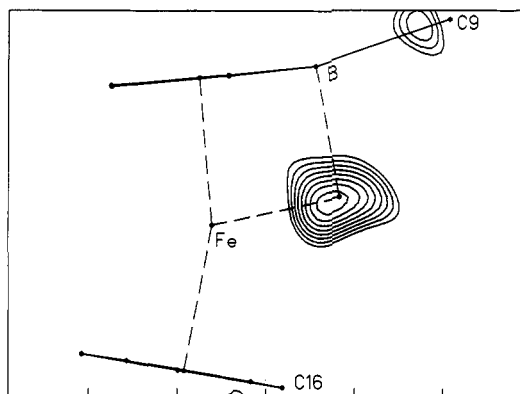


Figure 3. Difference-electron density map for the hydrogen atom of **1d** presented with isoelectron lines (outer line $0.30 \times 10^{-6} \text{ e/pm}^3$, steps in $0.05 \times 10^{-6} \text{ e/pm}^3$).

Table 4. Selected Bond Distances and Bond Angles for **1f**

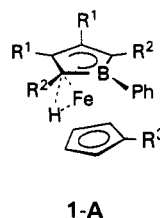
(a) Bond Distances (pm)			
Metal-Ligand and Borole			
Fe-B	215.5(2)	Fe-C1	210.1(2)
Fe-H	147.5(23)	Fe-C2	205.8(2)
B-H	146.1(26)	Fe-C3	206.0(2)
		Fe-C4	211.0(2)
B-C1	157.8(2)	B-C7	159.0(3)
C1-C2	141.0(3)	C1-C5	150.4(3)
C2-C3	143.9(3)	C4-C6	150.2(3)
C3-C4	141.2(3)		
B-C4	156.7(3)		
Cp Ring C13...C17			
Fe-C _{min}	205.1(2)	C-C _{min}	139.5(3)
Fe-C _{max}	208.1(2)	C-C _{max}	142.6(3)
Fe-C _{av}	206.6	C-C _{av}	141.5
(b) Bond Angles (deg)			
Fe-H-B	94.5(14)	B-C1-C2	107.7(2)
C1-B-C4	102.3(1)	C1-C2-C3	111.1(2)
C1-B-C7	126.3(2)	C2-C3-C4	110.8(2)
C4-B-C7	127.1(2)	C3-C4-B	108.1(2)

The C-C bond lengths within the borole ring (141.4/143.7/142.7 pm for **1d** and 141.0/143.9/141.2 pm for **1f**) show that metal-to-ligand back-bonding into the diene region of the borole ring is less important than in Fe-(CO)₃(C₄H₄BPh) (**3a**) (142.6/141.7/143.5 pm).¹³ This is not unexpected for d⁶ systems, where back-bonding is generally less favorable than in d⁸ systems.¹⁶ On the other hand, the Fe-B distance (215.1(4) pm for **1d** and 215.5(2) pm for **1f**) is much shorter than for **3a** (228.6(2) pm).¹³

The most interesting feature of the structure is the position of the hydridic hydrogen atom. The Fe-H distance (147(3) pm for **1d** and 147.5(23) pm for **1f**) is similar to Fe-H distances found in classical iron hydride complexes such as *cis,mer*-FeH₂(H₂)(PEtPh₂)₃ (151.4(6) and 153.8(7) pm, determined by neutron diffraction at 27 K).¹⁷ The B-H distance (151(3) pm for **1d** and 146.1(26) pm for **1f**) is rather long for a three-center Fe-H-B bond (cf., e.g., Fe₂(B₃H₇)(CO)₆ with B-H = 127(4) and 137(4) pm and Fe-H = 156(4) and 166(4) pm for Fe-H-B, determined by X-ray diffraction¹⁸) and therefore does not represent unambiguous evidence for three-center bonding. However, there are several details which warrant the presence of a B-H bonding interaction. A cross section

through the approximate mirror plane of the sandwich moiety of **1d** (Figure 3) shows a pronounced bending of the hydrogen atom toward the boron atom. The slip distortion¹⁹ of the iron toward the diene region of the borole ring (2.1 pm for **1d** and 3.6 pm for **1f**) is unusually small (cf. 6.9 pm for **3a**¹³), thus holding the iron atom closer to the boron atom. The usual folding of the borole ring along the line C1,C4 and away from the metal is reduced and amounts to only 0.8 and 0.5° (cf. 6.1° for **3a**¹³). In addition, the sum of the bonding angles at the boron atom is slightly but significantly smaller than 360° (357.6° for **1d** and 355.7° for **1f**), with the phenyl group bending away from the hydridic hydrogen.

It could be argued that a disordered racemate of agostic enantiomers **1-A** would produce apparent lateral symmetry. However, a careful check of the difference Fourier



synthesis for **1d** that gave the position of the hydridic hydrogen did not show a significant elongation of the corresponding electron density in the direction perpendicular to the molecular mirror plane. Hence, we conclude the following: all evidence from two very similar structure determinations shows that the hydrides of type **1** possess the laterally symmetric ground state **1-G** ($\equiv 1$), which involves an Fe-H-B three-center interaction with weak B-H bonding.

Spectroscopic Characterization. The hydrides **1a,b,e**, without substituents at the 2,5-position, show temperature-dependent ¹H and ¹¹B NMR spectra which indicate the presence of two dynamic processes. At room temperature the ¹H NMR (80-MHz) spectrum for **1a** displays broadened signals for the 2,5-protons of the borole ring and the hydridic proton; fine structure due to the coupling between the borole protons cannot be discerned. When the temperature is raised, the signals of the 2,5-protons and of the hydridic proton coalesce at 333 K. Then a single signal emerges for these three protons which sharpens upon further heating up to the limit of beginning decomposition at 383 K. On the other hand, when the temperature is lowered, the signal of the hydridic proton sharpens and the expected pattern for an AA'BB' spin system with its characteristic fine structure⁸ appears for the borole protons. There is no appreciable direct ¹¹B-¹H coupling, as the line width of the hydridic hydrogen is rather small (e.g. for **1a**, 4 Hz at 243 K and 7 Hz at 193 K); in fact, this observation is not unexpected, as the B-H interaction will be mediated essentially by the 2p_z orbital of the boron with little admixture of s character at boron. The exchange of the 2,5-protons and the hydridic proton is an intramolecular process, as it is independent of the concentration of **1a**. Simulation of the dynamic NMR spectra establishes a free energy of activation $\Delta G^*_{333} = 17.0 \pm 0.7 \text{ kcal/mol}$ for **1a** and $16.7 \pm 0.7 \text{ kcal/mol}$ for **1b**.²⁰

(16) Elian, M.; Hoffmann, R. *Inorg. Chem.* 1975, 14, 1058.

(17) VanDerSluis, L. S.; Eckert, J.; Eisenstein, O.; Hall, J. H.; Huffman, J. C.; Jackson, S. A.; Koetzle, T. F.; Kubas, G. J.; Vergamini, P. J.; Caulton, K. G. *J. Am. Chem. Soc.* 1990, 112, 4831.

(18) Haller, K. J.; Andersen, E. L.; Fehlner, T. P. *Inorg. Chem.* 1981, 20, 309.

(19) The slip distortion is the distance between the geometric center of the heterocycle and the projection of the metal atom.

(20) The simulation was carried out with the program GEM-NMR by C. G. Kreiter and U. Seimet, University of Kaiserslautern.

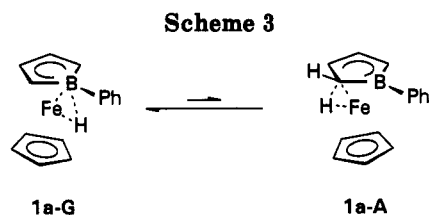


Table 5. Selected $\delta(^{11}\text{B})$ Data for the Hydrides 1a-f

compd	<i>T</i> (K)	$\delta(^{11}\text{B})$	compd	<i>T</i> (K)	$\delta(^{11}\text{B})$	
1a	203	-6.0	1c	299	-8.6	
	299	-3.5		1d	299	-8.7
	363	1.5		1e	299	-5.5
1b	213	-7.3	1f	299	-8.0	
	323	-5.7				
	383	-1.9				

Furthermore, the protons of **1a,b,e** that are not involved in the exchange process show a marked temperature dependence of their chemical shifts down to the practical low-temperature limit of 193 K (e.g. for **1a** $\delta(^1\text{H})$ 7.60 (H_o) and 4.03 (Cp) at 383 K versus $\delta(^1\text{H})$ 7.99 (H_o) and 3.66 (Cp) at 193 K). The ^{11}B NMR signal occurs at a very high field compared to that for non-hydridic borole sandwich complexes² (e.g. for $\text{CpCo}(\text{C}_4\text{H}_4\text{BPh})$ $\delta(^{11}\text{B})$ 18.0⁸) and, in addition, shows a significant shift to higher field at lower temperatures. In contrast to these observations, the spectra of dimethylated hydrides **1c,d** show no significant temperature dependence and their $\delta(^{11}\text{B})$ shifts are comparable to the shifts of **1a,b** at the lowest temperature. Some pertinent data are collected in Table 5.

These data indicate a fast equilibrium between at least two species for **1a,b,e**, with a ground-state species of type **1-G** (Scheme 3). As the higher energy isomer we propose the agostic species **1-A** with a much less shielded boron atom. The closely related $\text{MnH}(\text{CO})_3(\text{C}_4\text{H}_4\text{BPh})$ with $\delta(^{11}\text{B})$ 31.9 possesses an agostic ground-state structure, as found by low-temperature NMR.²¹ Related classical structures with boracyclopentenyl ligands also show deshielded boron, e.g. for $\text{CpNi}(\text{C}_4\text{H}_5\text{BPh})$ $\delta(^{11}\text{B})$ 35²² and for $\text{Co}(\text{CO})_2(\text{PMe}_3)(\text{C}_4\text{H}_5\text{BPh})$ $\delta(^{11}\text{B})$ 30.0.¹ If we assume $\delta(^{11}\text{B})$ -7.0 for **1a-G** (cf. Table 5) and $\delta(^{11}\text{B})$ 32 for **1a-A**, the boron shift of $\delta(^{11}\text{B})$ -3.4 at 299 K gives a rough estimate of 9% for the share of **1a-A** in a solution of **1a** at 299 K corresponding to $\Delta G = 1.4$ kcal/mol.

Within the framework of Scheme 3 the two enantiomers of **1a-A** are in rapid equilibrium via **1a-G**, that is, by a path for the proton on the endo side of the borole ring. It should be noted that this low-energy process conserves the identity of the hydridic proton. A migration of the proton $\delta\text{-exo-H}$ to C-2 across the exo face of the borole ligand also interconverts the two enantiomers of **1a-A** but, in addition, exchanges the 2,5-borole protons and the hydridic proton. It seems likely that this migration across the exo face is the mechanism of the above-described intramolecular exchange process. To gain further support for the existence of agostic isomers of type **1-A** and for the mechanisms just postulated, it seemed desirable to look at the bonding situation in the hydrides **1** more closely.

Electronic Ground-State Structure of $\text{CpFeH}(\text{C}_4\text{H}_4\text{BH})$. Using Hoffmann's fragment-MO approach,

(21) The low-temperature limiting ^{13}C NMR spectrum of $\text{MnH}(\text{CO})_3(\text{C}_4\text{H}_4\text{BPh})$ shows four different ring carbon atoms with a doublet of doublets for C-5 ($^1J = 161 \pm 5$ and 92 ± 5 Hz): Herberich, G. E.; Köffer, D. P. J.; Kreiter, C. G., unpublished results.

(22) Herberich, G. E.; Hausmann, I.; Hessner, B.; Negele, M. J. *Organomet. Chem.* 1989, 362, 259.

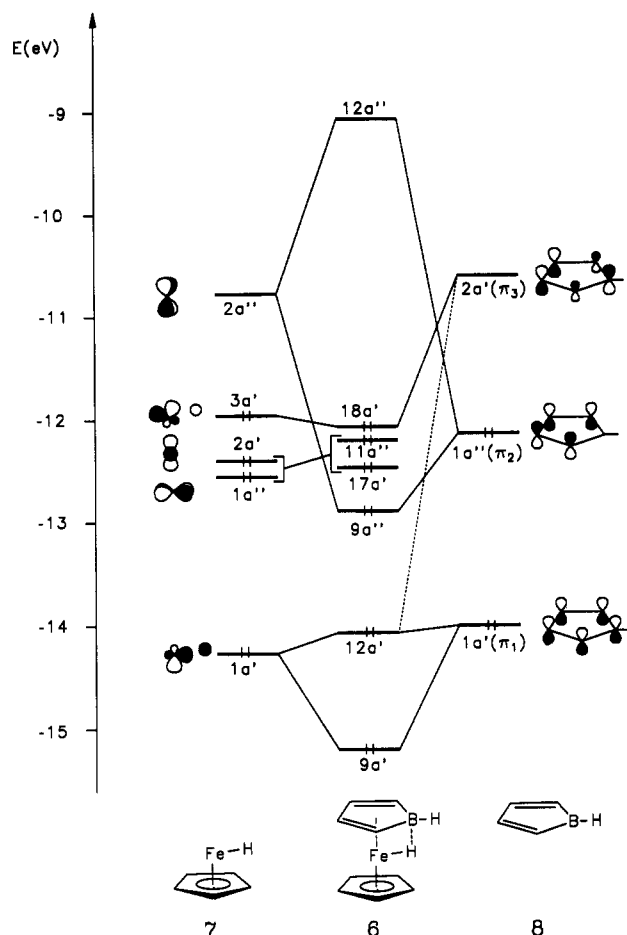


Figure 4. Frontier orbital diagram for $\text{CpFeH}(\text{C}_4\text{H}_4\text{BH})$ (**6**).

we derive the frontier MO's of $\text{CpFeH}(\text{C}_4\text{H}_4\text{BH})$ (**6**) from the CpFeH (**7**) fragment and the borole ligand $\text{C}_4\text{H}_4\text{BH}$ (**8**). The most important orbitals of **7** are shown on the left side of Figure 4. Going from lower to higher energy, one finds the $1a'$ level, which is mainly composed of the $1s$ orbital of the hydrogen atom and the iron $d_{z^2-y^2}$ orbital. In the localized picture it describes the Fe-H σ bond. The $1a'$ fragment MO is followed by the three metal-centered MO's $1a''$, $2a'$, and $3a'$. The last two can be described as linear combinations of the d_{z^2} , $d_{x^2-y^2}$, and d_{yz} iron orbitals, while $1a''$ is the d_{xy} orbital. The low-lying LUMO, $2a''$, is the d_{xz} orbital of the iron center.

Fragment **8** contributes two occupied π MO's ($1a'(\pi_1)$ and $1a''(\pi_2)$) together with a low-lying empty MO ($2a'(\pi_3)$) (see Figure 4, right). For the sake of clarity we omitted the σ MO's of **8** as well as all MO's localized on the Cp ring of **7** in Figure 4.

The frontier MO's of **6** arise from the interaction of both fragments, as shown in the center part of Figure 4. For their construction we make use of the noncrossing rule. The most important stabilizing contributions are achieved by the interactions of the HOMO and LUMO of both fragments. The interaction of the occupied $1a''(\pi_2)$ of **8** with the empty $2a''$ of **7** gives rise to the bonding level $9a''$ and the LUMO $12a''$ of **6**. The HOMO of **7** ($3a'$) interacts with π_3 of **8**, yielding $18a'$ (HOMO) and $19a'$ (not shown in Figure 4) of **6**. This interaction leads to a charge transfer from the iron to the borole ligand. This can best be seen from the net charges of the iron in **7** ($q(\text{Fe}) = -0.44$) and **6** ($q(\text{Fe}) = +0.10$). This change is due to metal-to-ligand back-bonding and to some extent to the three-center Fe-H-B interaction in **6**. The orbital $1a'$ of **7** (Fe-H

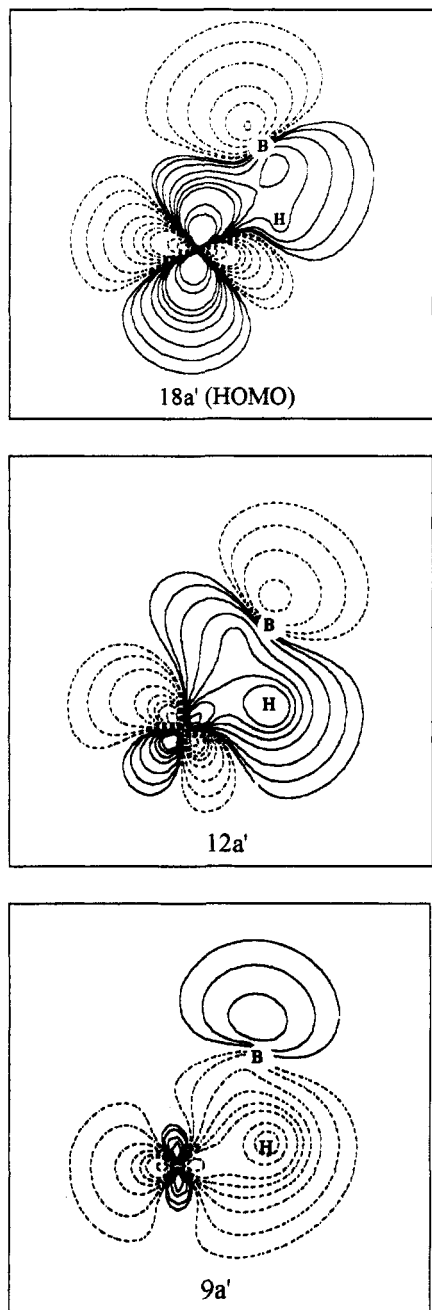


Figure 5. Contour plots of the orbitals 18a', 12a', and 9a' in the yz plane.

σ bond) interacts with 1a' (π_1) and 2a' (π_3) of 8, yielding 9a' and 12a' of 6. The interaction with the unoccupied 2a' (π_3) level allows an electron density transfer from the Fe-H σ bond to the borole ligand and describes the Fe-H-B bond. The contour plots of 18a', 12a', and 9a' are shown in Figure 5. In all three cases a mixing between 3d orbitals at the iron, the 1s orbital at the hydrogen, and the 2p orbital at the boron center can be seen.

Search for Tautomeric Structures and Dynamic Processes. In Figure 6 we have shown the total energy of 6 as a function of an angle α which describes the rotation of the hydrogen around the z axis starting from the yz plane ($\alpha = 0^\circ$). Energy values are calculated by using the extended Hückel method, changing only α and leaving all other parameters constant.

Due to the rotation of the hydrogen the stabilizing Fe-H-B interaction vanishes. At $\alpha = 140^\circ$ we obtain the local minimum 6-C. This local minimum is due to an

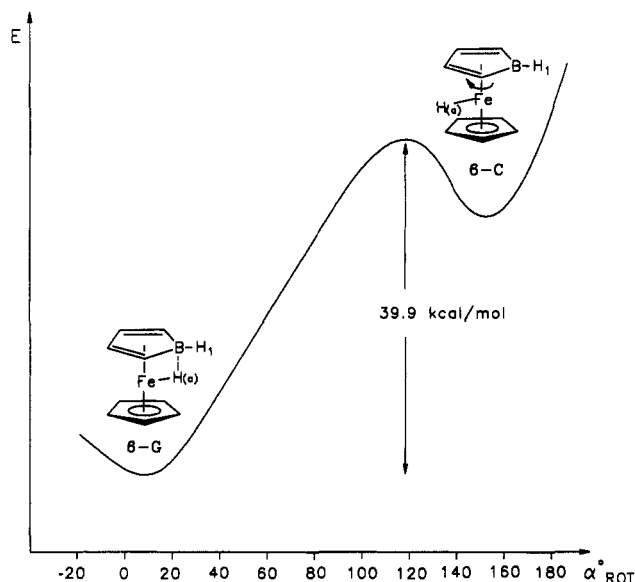


Figure 6. Total energy of 6 as a function of the rotational angle α (see text).

Table 6. Cyclic Voltammetry Data^a

complex	couple	E (V) ^b	ΔE (mV) ^c	i_c/i_a	v (V/s)	solvent
1a	+ / 0	0.72	<i>d</i>		0.1	DME
1a-A	0 / -	-0.76	<i>d</i>		0.05-1.0	
1a-G	0 / -	-2.03	<i>d</i>		0.05-1.0	
1d	+ / 0	0.68	<i>d</i>		0.1	DME
	0 / -	-2.30	70	0.97	0.02-0.5	
5a-	0 / -	-0.79	75	1.0	0.05-5	DME
	- / 2-	-2.25	<i>d</i>		0.1	DME

^a Data reported for platinum working electrode at room temperature; electrolyte concentration is 0.1 M. ^b Potentials are vs SCE; E° reported for reversible systems, peak potentials (E_p^c , E_p^s) for irreversible processes. ^c Peak separation, exceeds 60-70 mV for reversible signals in DME due to uncompensated iR drop. ^d Irreversible.

interaction between the hydrogen at the iron and the p_z AO at C-3. The energy difference between the global minimum 6-G and 6-C is predicted to be 36 kcal/mol. The activation energy for the reaction of 6-A to give 6-C is calculated to be 40 kcal/mol.

To rationalize the intramolecular proton exchange of 1a,b,e, we have carried out model calculations on 6. Since a rigorous treatment is not possible because of the shortcomings of the extended Hückel method with respect to the optimization of bond lengths, we changed only a few parameters. First, we move the hydrogen at C-2 of the borole ring, H2, away from the borole plane and we rotate the Fe-H bond by 70° out of the yz plane (points 1-6 in Figure 7). The energy can be reduced by moving the hydrogen at the iron atom (H(a)) to C-2 (points 7 and 10). The bending of H2 reduces the activation energy from 40 kcal/mol (Figure 6) to 27 kcal/mol (Figure 7). The calculated energy difference between 6-G and the agostic isomer 6-A amounts to 15 kcal/mol. In the following steps (11-16) we move H(a), H2, and H1 in such a way that at the end the boratacyclopentadiene species 6-B is obtained. For this movement an activation energy of 9.2 kcal/mol is estimated. The second intermediate 6-B is predicted at the same energy as 6-A. The migration of H2 to C-5 is analogous to the previous step (6-A to 6-B), and the migration of H5 to Fe is identical with the first step. If, however, H2 in 6-A is moved directly to C-5 without the detour via 6-B, an additional energy barrier of 33 kcal/mol is calculated. Hence, this "direct path" seems very unlikely.

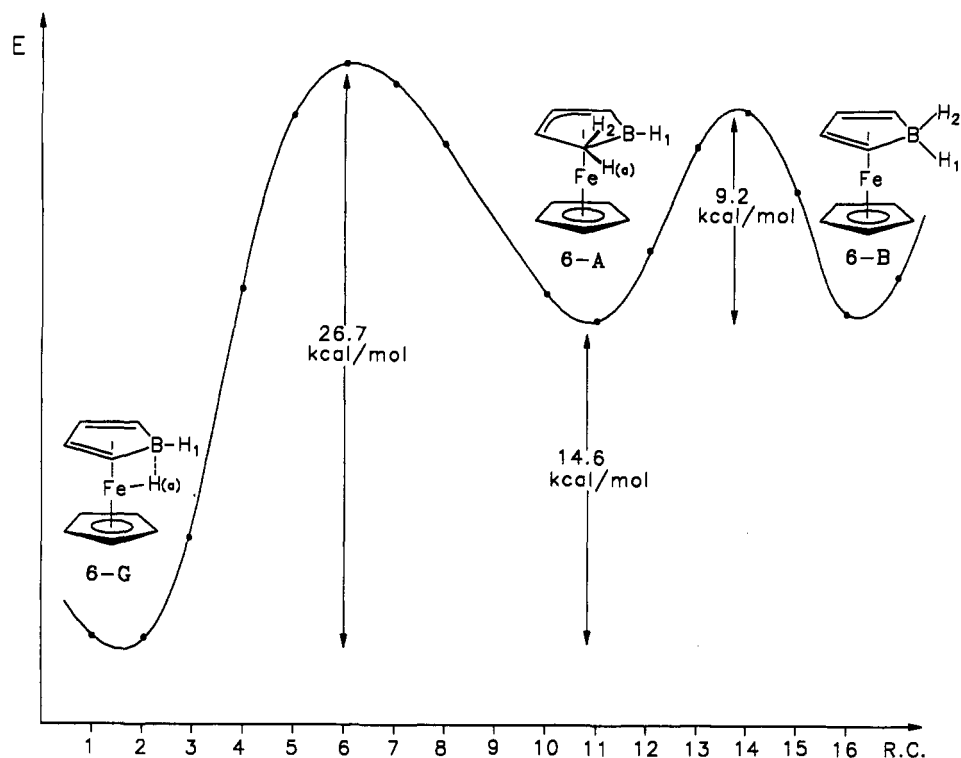


Figure 7. Total energy of 6 as a function of the reaction coordinate for hydrogen migration (see text).

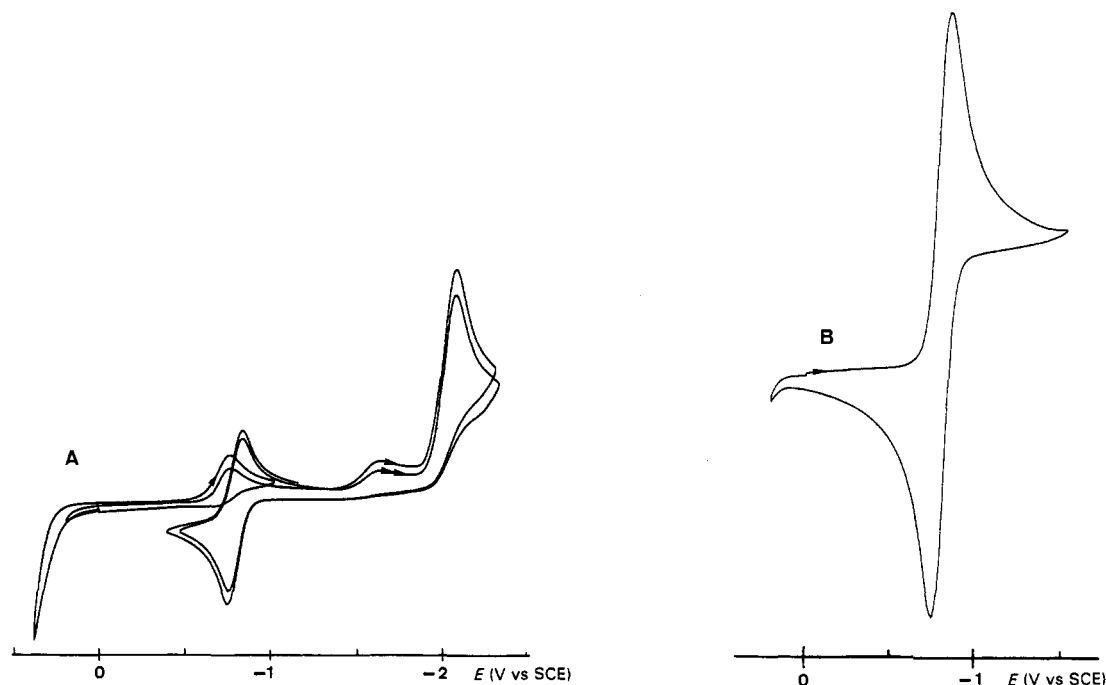


Figure 8. Cyclic voltammograms for 1a (A) and for 5a/5a⁻ (B).

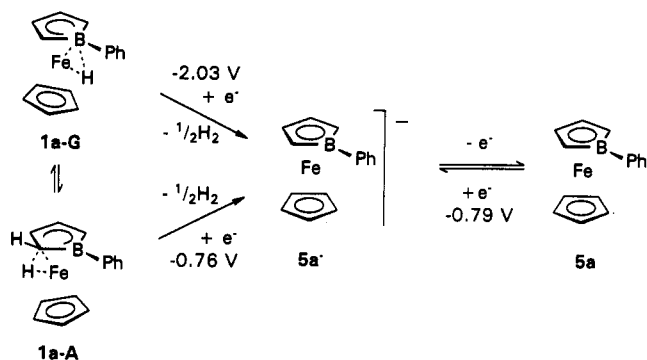
We also considered the tautomer (CpH)Fe(C₄H₄BH) (6-D) with the agostic interaction Fe-H-C(Cp). For this agostic isomer the calculated energy difference between 6-D and 6-G amounts to 25 kcal/mol, while the energy difference between 6-A and 6-G is predicted to be 15 kcal/mol.

Electrochemical Results and Identification of the 17e Complex CpFe(C₄H₄BPh) (5a) by EPR and Paramagnetic NMR Spectroscopy. Investigation of 1a by cyclic voltammetry showed a complex behavior (Figure 8, Table 6). On reducing 1a in Bu₄NPF₆/DME solution at room temperature, we observed two irreversible reduction peaks at -0.76 and -2.03 V. The reduction peak at -0.76

V exhibits reoxidation at -58 °C ($\nu = 0.2$ V/s), with i_a/i_c being 0.97. Both reductions yield the same product represented by the reversible oxidation wave at $E^\circ = -0.79$ V. The cyclic voltammogram of Na-5a shows a reversible oxidation wave at the same potential. These observations suggest that the irreversible reduction of 1a results in the formation of anion 5a⁻, via hydrogen abstraction from the short-lived intermediate 1a⁻, and that 5a⁻ shows a reversible oxidation to the paramagnetic species 5a (Scheme 4).

The anion 5a⁻ is very air-sensitive and undergoes fast oxidation with oxygen even at low temperature. Dilute solutions of 5a in THF can readily be generated, e.g. from [Li(TMEDA)]5a in THF by controlled oxidation with air

Scheme 4



(cf. NMR experiments below), and reduction with potassium regenerates 5a⁻. However, attempts to isolate 5a have failed so far. Frozen solutions of 5a display an EPR spectrum (100 K, glassy frozen THF-*d*₈, $g_{\parallel} = 3.05$ and $g_{\perp} = 1.97$).

The observation of two irreversible reduction processes is in agreement with the hypothesis of an equilibrium between the two isomers 1a-G and 1a-A. The first peak at -0.76 V is assigned to the reduction of 1a-A and the peak at -2.03 V to that of 1a-G. Bulk electrolysis of 1a at -1.0 V effected complete conversion to 5a⁻; in a subsequent cyclic voltammogram the reduction peak at -2.03 V had also disappeared. In striking contrast to 1a the 2,3,4,5-tetramethyl derivative 1d shows a single reversible reduction at -2.30 V. This process corresponds to the reduction of 1a-G; the four additional methyl groups of 1d effect a cathodic shift of the reduction and a stabilization of the reduced species 1d⁻ in agreement with general trends.²³

By stepwise oxidation of ¹H NMR samples of [Li(TMEDA)]5a⁹ in THF-*d*₈ with air an increasing shift of most signals is observed which is caused by the paramagnetism of 5a. This process comes to an end when the formation of 5a is completed and can be reversed by reduction of 5a at a potassium mirror in the sample tube (Figure 9, Table 7). The anion 5a⁻ is stable for weeks in contact with metallic potassium.

The observation of only one signal for every set of equivalent protons in diamagnetic 5a⁻, paramagnetic 5a, and mixtures of both species indicates a rapid symmetrical electron transfer between these two species. Thus, the observed chemical shift δ_{obs} for mixtures of 5a/5a⁻ is the mean of the chemical shifts δ_{dia} and δ_{para} weighted with the mole fractions f_{d} and f_{p} of diamagnetic 5a⁻ and paramagnetic 5a, respectively (eq 1). Hence, δ_{obs} is linearly

$$\delta_{\text{obs}} = f_{\text{d}}\delta_{\text{dia}} + f_{\text{p}}\delta_{\text{para}} \quad (1)$$

$$\delta_{\text{p}} = \delta_{\text{para}} - \delta_{\text{dia}} \quad (2)$$

dependent on the paramagnetic mole fraction f_{p} . This relationship allows an unambiguous correlation between the spectra of both redox states, and in this way the paramagnetic spectra of 5a can be assigned easily (Table 8).²⁴ The difference $\delta_{\text{para}} - \delta_{\text{dia}}$ represents the paramagnetic shift δ_{p} (eq 2).

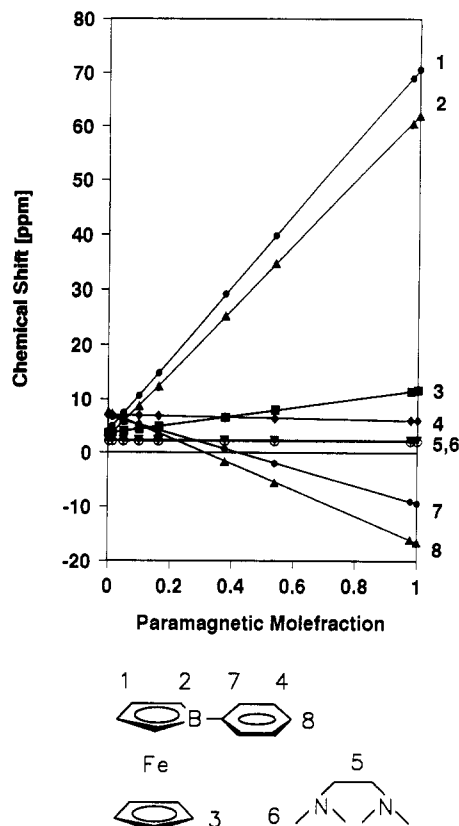


Figure 9. Chemical shifts δ_{obs} for 5a/5a⁻ as a function of paramagnetic mole fraction f_{p} .

Table 7. Chemical Shifts δ_{obs} (ppm) for ¹H NMR Signals as a Function of the Paramagnetic Mole Fraction f_{p}

f_{p}	signal ^a							
	1	2	3	4	5	6	7	8
0.000	4.03	2.82	3.61	7.05	2.30	2.15	6.92	7.65
0.013	4.93	3.70	3.73	7.03	2.30	2.15	6.65	7.27
0.050	7.45	5.95	3.98	7.00	2.30	2.15	6.04	6.35
0.100	10.65	8.70	4.37	6.95	2.30	2.15	5.24	5.24
0.162	14.80	12.42	4.87	6.88	2.30	2.15	4.21	3.60
0.377	29.2	25.3	6.6	6.60	2.30	2.15	0.65	-1.70
0.538	39.8	34.8	8.0	6.43	2.30	2.15	-1.98	-5.60
0.978	69.0	60.5	11.5	6.08	2.30	2.15	-9.0	-16.0
1.000	70.6	62.0	11.7	6.06	2.30	2.15	-9.4	-16.5

^a For signal designation see Figure 9.

Table 8. Paramagnetic Shifts (ppm) and Line Widths (Hz) for ¹H NMR Signals of 5a

	signal ^a							
	1	2	3	4	5	6	7	8
δ_{p}^b	66.6	59.2	8.1	1.0	0	0	-16.3	-24.2
LW_{p}^c	680	470	290	0	0	0	20	46

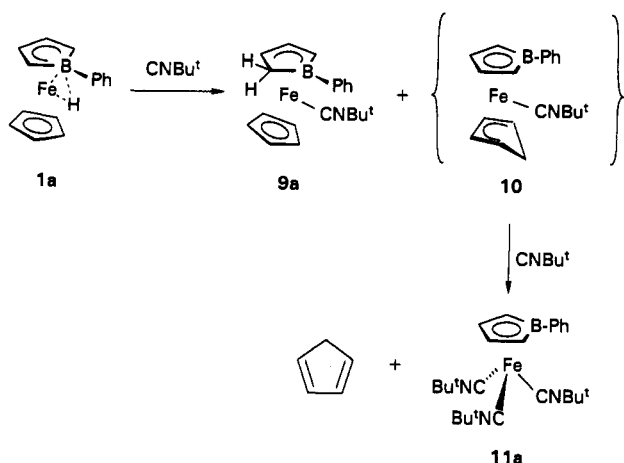
^a For signal designation see Figure 9. ^b See eq 2. ^c $LW_{\text{p}} = [\text{line width } (f_{\text{p}} = 1)] - [\text{line width } (f_{\text{p}} = 0)]$.

All protons of 5a show the paramagnetic shift δ_{p} with respect to the diamagnetic line positions of 5a⁻ (Table 8), while the ligand TMEDA of the gegenion Li⁺ remains unaffected. Within 5a the paramagnetic shifts vary widely. The strong dispersion of line width for the paramagnetic NMR signals indicates that there is more than one cause for this situation.²⁵ This point is presently under study.

(24) (a) Köhler, F. H.; Zenneck, U.; Edwin, J.; Siebert, W. *J. Organomet. Chem.* 1981, 208, 137. (b) Zwecker, J.; Kuhlmann, T.; Pritzkow, H.; Siebert, W.; Zenneck, U. *Organometallics* 1988, 7, 2316. (c) Stephan, M.; Davis, J. H.; Meng, X.; Chase, K. J.; Hauss, J.; Zenneck, U.; Pritzkow, H.; Siebert, W.; Grimes, R. N. *J. Am. Chem. Soc.* 1992, 114, 5214.

(23) (a) Koelle, U.; Khouzami, F. *Angew. Chem.* 1980, 92, 658; *Angew. Chem., Int. Ed. Engl.* 1980, 19, 640. (b) Richardson, D. E.; Ryan, M. F.; Khan, M. N. I.; Maxwell, K. A. *J. Am. Chem. Soc.* 1992, 114, 10482.

Scheme 5



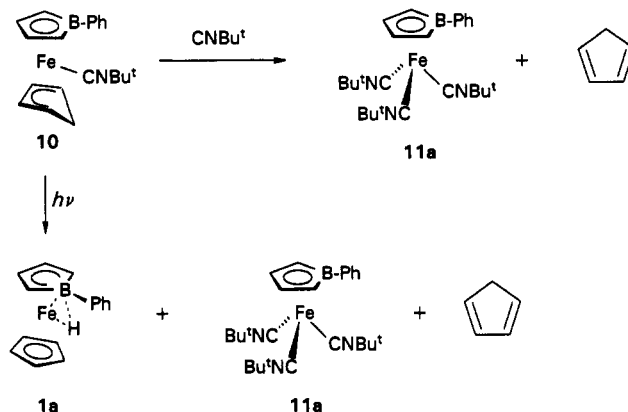
Reactivity of 1a. Chemical Evidence for the Existence of the Agostic Isomer 1a-A. Many agostic compounds add 2e donors such as CO or isocyanides with a concomitant shift of the agostic hydrogen atom.²⁶ We therefore investigated the reaction of 1a with CNBu^t . When the reaction was monitored by NMR spectroscopy, three products were seen after a few hours at room temperature (Scheme 5). Treating 1a with an approximately equimolar amount of CNBu^t (1.1 equiv) yielded a mixture of unconsumed 1a (29%), the addition product $\text{CpFe}(\text{CNBu}^t)(\text{C}_4\text{H}_5\text{BPh})$ (9a; 53%), and $\text{Fe}(\text{CNBu}^t)_3(\text{C}_4\text{H}_4\text{BPh})$ (11a) together with free cyclopentadiene (each 18%). With an excess of CNBu^t 1a was consumed completely. The products 9a (51%) and 11a (49%) did not react any further with unconsumed isocyanide. While 11a is a robust compound which could readily be isolated, 9a decomposed on attempted purification by chromatography. Our observations suggest two parallel reaction channels, one of these giving the observed product 9a while the other one, via the hypothetical intermediate 10, forms 11a and cyclopentadiene.

We repeated the above experiment with deuterated 1a. Treatment of the trideutero complex 1a- d_3 (95% deuteration) with excess CNBu^t gave 9a- d_3 (73%) and 11a- d_2 and $\text{C}_5\text{H}_5\text{D}$ (each 27%). The NMR spectra of the complex products showed the deuterium to be in the 2-/5-position of the C_4B ring ligands only. Cyclopentadiene was captured with maleic acid anhydride as the Diels-Alder adduct 12. Examination of 12 by mass spectroscopy showed the presence of just one deuterium label (85%). Thus, there is essentially no isotopic scrambling.

Shining light onto the solution in presence of excess CNBu^t caused a slow conversion of 9a to 11a. Light-induced primary dissociation of 9a is thought to give 1a (via 1a-A) and CNBu^t , which then can recombine to form 9a and 11a (via 10) until all material is transformed into the final product 11a.

Scheme 5 implies that the proposed intermediate 10 should readily react with CNBu^t to give 11a and cyclopentadiene. Complex 10 could be prepared independently from $\text{Fe}(\text{CO})_2(\text{CNBu}^t)(\text{C}_4\text{H}_4\text{BPh})^9$ by irradiation in the presence of cyclopentadiene. When 10 was then treated with an excess of CNBu^t , very fast degradation took place

Scheme 6



to give 11a and free cyclopentadiene (Scheme 6). Exposing a solution of the cyclopentadiene complex 10 in C_6D_6 to light induces disproportionation and produces 1a (60%), 11a (40%), and free cyclopentadiene (Scheme 6). Again the light-induced primary dissociation of 10 will give 1a and CNBu^t followed by thermal degradation of more cyclopentadiene complex 10 by the liberated CNBu^t .

The 2,5-dimethyl derivative 1c reacts with CNBu^t in the same way as 1a, albeit at a much lower rate. While the reaction of 1a took a few hours at room temperature, the reaction of 1c required 30 days and afforded the η^4 -boracyclopentenyl complex 9c (25%) and the tris(isocyanide) complex 11c (75%).

Discussion

(Borole)(cyclopentadienyl)iron hydrides 1 are a new family of complex iron hydrides. The laterally symmetric ground-state structure 1-G of the 2,5-dialkylated members (1c,d,f-h) is unambiguously established by our X-ray structural work. While the B-H distances are rather long for Fe-H-B three-center bonding, several structural details provide evidence for the presence of a presumably weak Fe-H-B three-center interaction; this interpretation is strengthened by the analysis of the bonding situation on the basis of extended Hückel calculations. For the 2,5-unsubstituted derivatives (1a,b,e) tautomeric structures (the ones of type 1-A) are very close in energy. Comparison of the low-temperature NMR data shows, however, that these derivatives possess the same type of ground-state structure 1-G.

The temperature dependence of the chemical shift data for the 2,5-unsubstituted derivatives required the assumption of an equilibrium between at least two tautomers. The choice of agostic isomers of type 1-A as higher energy tautomers cannot be stringently deduced from the NMR spectra but merely relies on good agreement with our spectral observations and on general chemical intuition.

At this point our extended Hückel calculations were used to find energy minima for the location of the hydrogen atom during its rotation around the axis of the borata-ferrocene sandwich and the migration across the exo face of the borole ligand. Three important minima were found, one (6-G) for the ground state, one (6-A) corresponding to an agostic structure of type 1-A, and a second one (6-B) corresponding to the structure of a borata-2,4-cyclopentadiene complex. We note here that a related complex with a 1-methyl-1-phenylborata-2,4-cyclopentadiene ligand, $\text{Li}[\text{Fe}(\text{CO})_3(\text{C}_4\text{H}_4\text{BMePh})]$, has recently been observed experimentally as a low-temperature ($< -50^\circ\text{C}$) solution

(25) Keller, H. J. In *NMR Basic Principles and Progress*; Diehl, P., Fluck, E., Kosfeld, R., Eds.; Springer-Verlag: Berlin, 1970; Vol. 2, p 53.

(26) (a) Ittel, S. D.; Van-Catledge, F. A.; Jesson, J. P. *J. Am. Chem. Soc.* 1979, 101, 6905. (b) Lamanna, W.; Brookhart, M. *J. Am. Chem. Soc.* 1981, 103, 989.

species.¹¹ The calculations therefore support our interpretation of the NMR spectra of the hydrides 1.

Two further minima, 1-C and 1-D, were found which lie at rather high energies and therefore are of little importance. In case of isomer 1-D it is also experimentally clear from the ¹H NMR spectra that this isomer does not contribute to the tautomeric equilibrium of 1a, as the Cp signal of 1a does not show any line broadening.

Finally, in the reaction of 1a and 1c with CNBu^t the hydridic hydrogen is shifted to C2 of the borole ligand or alternatively to a Cp carbon atom (Scheme 5). This process is intramolecular, as no isotopic scrambling is observed. The addition of a 2e donor is a characteristic reaction of many agostic compounds.²⁶ In this vein we assume that the agostic isomers 1-A and 1-D respectively act as intermediates in the isonitrile addition reaction.

Experimental Section

General Procedures. Reactions were carried out under an atmosphere of dinitrogen by means of conventional Schlenk techniques. Pentane and hexane were distilled from Na/K alloy, toluene and ethereal solvents were distilled from sodium benzophenone ketyl, and methylene chloride was distilled from CaH₂. Alumina for chromatography (Woelm) was heated under a high vacuum at 300 °C and deactivated (7% H₂O, deoxygenated) after cooling. Melting points were measured in sealed capillaries and are uncorrected. Elemental analyses were performed by Analytische Laboratorien, D-51753 Engelskirchen, FRG.

NMR spectra were recorded on a Bruker WH 270 PFT spectrometer (¹H, 270 MHz; ¹³C, 67.88 MHz), a Bruker WP 80 PFT spectrometer (¹H, 80 MHz), and a JEOL NM-PS-100 spectrometer (¹¹B, 32.08 MHz). The digital resolution was <0.5 Hz/point for ¹H and <1.0 Hz/point for ¹³C spectra; half-widths of broad signals are given in parentheses. EPR spectra were recorded on a Bruker ESP 300 E spectrometer. DPPH (*g* = 2.0036) was used as a standard for determination of the *g* value. The paramagnetic NMR spectra were measured on a JEOL JNM GX 270 spectrometer. Infrared spectra were recorded on a Perkin-Elmer 842 spectrometer.

Preparation of 3b. A solution of 5.4 g (31.8 mmol) of 3,4-dimethyl-1-phenyl-3-borolene¹² (2b) and 2.1 mL (15.9 mmol) of Fe(CO)₅ in 150 mL of THF was irradiated for 7 days. The color of the solution changed from yellow to dark red. The reaction was monitored by IR spectroscopy. At the end of the reaction the solution was refluxed for 1 h. The solution was concentrated to 50 mL; then the same volume of alumina was added, and all volatiles were removed. The red, dry, solid material was transferred to a short column (4 cm wide) already charged with alumina to a height of 10 cm. The product was eluted with 500 mL of pentane. Crystallization of the product from 100 mL of pentane at -30 °C gave 3b (2.25 g, 46%).

3b: yellow, almost air-stable needles; mp 101 °C; dec pt ca. 300 °C; MS *m/z* (*I*_{rel}) 308 (50, M⁺), 224 (100, M⁺ - 3 CO); IR (hexane, cm⁻¹) 2060 s (CO), 2002 s (CO), 1990 s (CO); ¹H NMR (CDCl₃) δ 7.60 (m, 2 H_o), 7.28 (m, 2 H_m + H_p), borole 3.63 (s, 2/-5-H) and 2.12 (s, 3/-4-Me); ¹¹B NMR (CDCl₃) δ 19.1; ¹³C NMR (CDCl₃) δ 211.2 (s, 3 CO), 134.9 (d, ¹J = 155 Hz, 2 C_o), 128.6 (d, ¹J = 159 Hz, C_p), 127.8 (d, ¹J = 157 Hz, 2 C_m), borole 112.4 (s, C-3/-4), 77 (d br, C-2/-5, partly hidden by CDCl₃ signal), and 15.1 (q, ¹J = 128 Hz, 2/-5-Me). Anal. Calcd for C₁₅H₁₃BF₂O₃: C, 58.51; H, 4.26. Found: C, 58.46; H, 4.37.

Preparation of 4b. A solution of 3b (328 mg, 1.24 mmol) and 1.0 mL of cyclopentadiene (12.4 mmol) in 80 mL of hexane was irradiated for 5 h. The reaction was monitored by IR spectroscopy. The solution was concentrated in vacuo and chromatographed on alumina. After elution of a first yellow band with 3b an orange eluate with 4b and 1b was collected. Crystallization at -80 °C and a second chromatography at -20 °C yielded 4b (169 mg, 46%).

4b: sensitive brown powder; MS *m/z* (*I*_{rel}) 318 (39, M⁺), 290 (100, M⁺ - CO); IR (hexane, cm⁻¹) 1979 s, 1977 s; ¹H NMR (C₆D₆) δ 8.05 (m, 2 H_o), 7.48 (m, 2 H_m + H_p), borole 2.59 (s, 2/-5-H) and 1.53 (s, 3/-4-Me), C₆H₆ 4.90 (m, 2/-3-H), 2.87 (m, 1/-4-H), 2.09 (dm, ²J = 14 Hz, 5endo-H), and 1.48 (d, ²J = 14 Hz, 5exo-H); ¹¹B NMR (CDCl₃) δ 15.3.

Preparation of 1b. A solution of 3b (2.10 g, 6.8 mmol) and 6.2 mL (75.8 mmol) of cyclopentadiene in 150 mL of hexane was irradiated for 14 h. The reaction was monitored by IR spectroscopy. After filtration and concentration in vacuo crystallization at -30 °C gave 1b (1.15 g, 58%).

1b: very air-sensitive orange-red crystals; mp 46 °C dec; MS *m/z* (*I*_{rel}) 290 (100, M⁺), 212 (100, M⁺ - C₆H₆); ¹H NMR (toluene-*d*₈, -70 °C) δ 7.87 (m, 2 H_o), 7.31 (m, 2 H_m + H_p), 3.66 (s, Cp), borole 2.76 (s br (6.5 Hz), 2/-5-H), 1.90 (s, 3/-4-Me), and -5.56 (s br (8.7 Hz), FeH); ¹H NMR (toluene-*d*₈, 32 °C) δ 7.77 (m, 2 H_o), 7.28 (m, 2 H_m + H_p), 3.84 (s, Cp), borole 2.48 (s br (17 Hz), 2/-5-H) and 1.98 (s, 3/-4-Me), -5.25 (s br (30 Hz), FeH); in a spin saturation transfer experiment, homodecoupling at δ -5.25 results in intensity decrease at δ 2.48; ¹H NMR (toluene-*d*₈, 110 °C) δ 7.61 (m, 2 H_o), 7.17 (m, 2 H_m + H_p), 3.91 (s, Cp), borole + hydride 2.03 (s, 3/-4-Me) and -0.21 (s br (27 Hz), 2/-5-H + FeH); ¹¹B NMR (CDCl₃) δ = 6.8; ¹³C NMR (toluene-*d*₈, -65 °C) δ 138.7 (s, C_i), 134.8 (d, ¹J = 158 Hz, 2 C_o), 127.4 (d, ¹J = 158 Hz, 2 C_m), 126.5 (d, ¹J = 160 Hz, C_p), 76.4 (d, ¹J = 170 Hz, Cp), borole 108.2 (s, C-3/-4), 68.4 (d, ¹J = 153 Hz, C-2/-5), and 17.5 (q, ¹J = 126 Hz, 3/-4-Me); ¹³C NMR (toluene-*d*₈, 27 °C) δ 135.0 (d, ¹J = 159 Hz, 2 C_o), 127.5 (d, ¹J = 158 Hz, 2 C_m), 126.5 (d, ¹J = 160 Hz, C_p), 76.2 (d, ¹J = 170 Hz, Cp), borole 107.6 (s, C-3/4), 68.0 (d br, C-2/5), and 17.2 (q, ¹J = 126 Hz, 3/-4-Me). Anal. Calcd for C₁₇H₁₉BFe: C, 70.41; H, 6.60. Found: C, 70.14; H, 6.56.

Preparation of 1e. By the same method 3a¹³ (2.60 g, 9.30 mmol) and 9.3 mL (93 mmol) of methylcyclopentadiene gave 1e (1.04 g, 40%).

1e: red-brown powder, mp 31 °C dec; thermally labile, very sensitive to air and moisture; MS *m/z* (*I*_{rel}) 276 (94%, M⁺), 198 (100, M⁺ - C₆H₆), 170 (14, 198 - C₂H₂); ¹H NMR (C₆D₆) δ 7.90 (m, 2 H_o), 7.34 (m, 2 H_m + H_p), borole 5.32 (s br (7 Hz), 3/-4-H) and 2.65 (s br (13 Hz), 2/-5-H), C₆H₄Me 3.92 (s, 4 H) and 1.46 (s, Me), -4.44 (s br (22 Hz), FeH); ¹¹B NMR (C₆D₆) δ -5.5; ¹³C NMR (C₆D₆) δ 135.6 (d, ¹J = 155 Hz, 2 C_o), signals of C_m and C_p hidden, borole 91.6 (d, ¹J = 167 Hz, C-3/-4) and 67.2 (d br, C-2/-5), C₆H₄Me 75.5 (d, ¹J = 173 Hz, C-3/-4), 73.4 (d, ¹J = 178, C-2/-5), and 14.4 (q, ¹J = 128 Hz, Me).

Preparation of 1c,d,f. To a solution of 1a,b,e (2.00 mmol) in 50 mL of THF were added iodomethane (0.37 mL, 6.00 mmol) and an excess of NaH. The solution was stirred until the evolution of gas ceased (12 h). Removal of the solvent, extraction of the residue with hexane, filtration through alumina, and crystallization from a concentrated solution at -78 °C afforded the product.

1c: red, air-stable crystals (44%); mp 82 °C; dec pt >160 °C; MS *m/z* (*I*_{rel}) 290 (100, M⁺), 274 (94, M⁺ - CH₄), 212 (94, M⁺ - C₆H₆); ¹H NMR (toluene-*d*₈, -80 °C) δ 8.04 (m, 2 H_o), 7.49 (m, 2 H_m + H_p), 3.66 (s, Cp), borole 4.94 (s, 3/-4-H) and 1.45 (s, 2/-5-Me), -5.78 (s br (5 Hz), FeH); ¹¹B NMR (toluene-*d*₈, 32 °C) δ 7.82 (m, 2 H_o), 7.38 (m, 2 H_m + H_p), 3.96 (s, Cp), borole 5.08 (s, 3/-4-H) and 1.37 (s, 2/-5-Me), -5.74 (s br (15 Hz), FeH); ¹H NMR (toluene-*d*₈, 110 °C) δ 7.81 (m, 2 H_o), 7.34 (m, 2 H_m + H_p), 4.08 (s, 3/-4-H + Cp), 1.35 (s, 2/-5-Me), -5.70 (s br (40 Hz), Fe H); ¹¹B NMR (CDCl₃) δ -8.6; ¹³C NMR (CD₂Cl₂, -80 °C) δ 140.4 (s, C_i), 135.5 (d, ¹J = 155 Hz, 2 C_o), 127.9 (d, ¹J = 157 Hz, 2 C_m), 126.5 (d, ¹J = 159 Hz, C_p), 75.7 (dm, ¹J = 179 Hz, Cp), borole 89.3 (d, ¹J = 165 Hz, C-3/-4), 88.4 (s, C-2/-5), 18.0 (q, ¹J = 125 Hz, 2/-5-Me); ¹³C NMR (CD₂Cl₂, 20 °C) δ 135.7 (d, ¹J = 155 Hz, 2 C_o), 127.8 (d, ¹J = 164 Hz, 2 C_m), 126.3 (d, ¹J = 159 Hz, C_p), 75.7 (dm, ¹J = 178 Hz, Cp), borole 89.7 (s, C-3/-4), 17.7 (q, ¹J = 126 Hz, 2/-5-Me). Anal. Calcd for C₁₉H₂₃BFe: C, 70.41; H, 6.60. Found: C, 70.01; H, 6.79.

1d: red air-stable crystals (89%); mp 104 °C; dec pt >180 °C; MS *m/z* (*I*_{rel}) 318 (85, M⁺), 302 (58, M⁺ - CH₄), 240 (100, M⁺ - C₆H₆); ¹H NMR (toluene-*d*₈, -75 °C) δ 7.96 (m, 2 H_o), 7.22 (m,

2 H_m + H_p), 3.48 (s, Cp), borole 1.77 (s, 3-/4-Me), 1.34 (s, 2-/5-Me), and -6.58 (s br (7 Hz), FeH); ¹H NMR (toluene-*d*₆, 20 °C) δ 7.86 (m, 2 H_o), 7.19 (m, 2 H_m + H_p), 3.71 (s, Cp), borole 1.91 (s, 3-/4-Me) and 1.31 (s, 2-/5-Me), -6.49 (s br (15 Hz), FeH); ¹H NMR (toluene-*d*₆, 110 °C) δ 7.78 (m, 2 H_o), 7.19 (m, 2 H_m + H_p), 3.82 (s, Cp), borole 2.01 (s, 3-/4-Me) and 1.30 (s, 2-/5-Me), -6.43 (s br (37 Hz), FeH); ¹¹B NMR (CDCl₃) δ -8.7; ¹³C NMR (CD₂Cl₂, -80 °C) δ 140.9 (s, C_o), 135.7 (d, ¹J = 155 Hz, 2 C_o), 127.9 (d, ¹J = 157 Hz, 2 C_m), 126.3 (d, ¹J = 159 Hz, C_p), 77.3 (dm, ¹J = 178 Hz, Cp), borole 105.1 (s, C-3/-4), 84.4 (s, C-2/-5), 15.3 (q, ¹J = 125 Hz, 2 Me), and 13.7 (q, ¹J = 126 Hz, 2 Me); ¹³C NMR (CD₂Cl₂, 20 °C) δ 136.0 (d, ¹J = 155 Hz, 2 C_o), 127.7 (d, ¹J = 156 Hz, 2 C_m), 126.1 (d, ¹J = 159 Hz, C_p), 77.4 (dm, ¹J = 178 Hz, Cp), borole 105.2 (s, C-3/-4), 15.0 (q, ¹J = 125 Hz, 2 Me), and 13.4 (q, ¹J = 126 Hz, 2 Me). Anal. Calcd for C₁₉H₂₃BF₂: C, 71.75; H, 7.23. Found: C, 71.66; H, 7.30.

1f: red, air-stable crystals (78%); mp 51 °C dec; MS *m/z* (*I*_{rel}) 304 (100, M⁺), 288 (96, M⁺ - CH₄), 273 (38, 288 - Me), 226 (95, M⁺ - C₆H₆), 224 (93, M⁺ - C₅H₅Me), 211 (47, 226 - Me), 209 (33, 211 - H₂), 144 (32, C₆H₅BF₂⁺), 132 (32, C₆H₅BF₂⁺); ¹H NMR (CDCl₃) δ 7.67 (m, 2 H_o), 7.28 (m, 2 H_m + H_p), borole 5.32 (s, 3-/4-H) and 1.38 (s, 2-/5-Me), C₆H₅Me 4.31 (s, 4 H) and 1.91 (s, Me), -5.79 (s br (14 Hz), FeH); ¹¹B NMR (CDCl₃) δ -8.0; ¹³C NMR (CDCl₃) δ 135.3 (d, ¹J = 162 Hz, 2 C_o), 127.4 (d, ¹J = 157 Hz, 2 C_m), 125.9 (d, ¹J = 155 Hz, C_p), borole 90.3 (d, ¹J = 164 Hz, C-3/-4) and 17.2 (q, ¹J = 125 Hz, 2-/5-Me), C₆H₅Me 76.0 (C-3/-4), 74.3 (d, ¹J = 177 Hz, C-2/-5), and 14.2 (q, ¹J = 129 Hz, Me). Anal. Calcd for C₂₀H₂₆BF₂: C, 71.11; H, 6.96. Found: C, 71.01; H, 7.06.

Preparation of 1g. NaH (0.150 g, 6.25 mmol) was added to a solution of **1a** (0.261 g, 1.00 mmol) in 40 mL of THF. After the mixture was stirred for 15 min at room temperature, 6-iodo-1-hexene (0.464 g, 2.20 mmol) was added and stirring was continued for 72 h. The solvent was removed, and the red residue was dissolved in Et₂O. Filtration and chromatography on alumina (20-cm column) gave a red band with **1g** (0.264 g, 62%), which was isolated by removing the solvent.

1g: red, slightly air-sensitive oil; MS *m/z* (*I*_{rel}) 426 (100, M⁺); ¹H NMR (C₆D₆) δ 7.82 (m, 2 H_o), 7.36 (m, 2 H_m + H_p), 4.08 (s, Cp), borole 5.18 (s, 3-/4-H), hexenyl 5.4-6.0 (m, 2 5-H), 4.7-5.2 (m, 4 6-H), and 0.76-2.34 (m, 8 CH₂), -6.13 (s br (11 Hz), FeH); ¹¹B NMR (C₆D₆) δ -5.6; ¹³C NMR (C₆D₆) δ 135.8 (d, ¹J = 155 Hz, 2 C_o), 127.6 (d, ¹J = 156 Hz, 2 C_m), signal of C_p hidden, 74.9 (d, ¹J = 178 Hz, C_p), borole 94.4 (s br (125 Hz), C-2/-5) and 88.0 (d, ¹J = 164 Hz, C-3/-4), hexenyl 139.1 (d, ¹J = 150 Hz, C-5), 114.4 (t, ¹J = 155 Hz, C-6), 33.8 (t, ¹J = 125 Hz, C-4), 32.0 (t, ¹J = 123 Hz, C-1), 31.9 (t, ¹J = 126 Hz, C-3), and 30.9 (t, ¹J = 124 Hz, C-2).

Preparation of 1h. As described above, **1a** (0.461 g, 1.77 mmol) in 25 mL of THF was stirred with NaH and (iodomethyl)cyclopropane for 96 h. Chromatographic workup first gave a red band with 15 mg of an unidentified product that did not exhibit allylic NMR signals and then second a red band with **1h** (0.30 g, 46%).

1h: red, slightly air-sensitive oil; MS *m/z* (*I*_{rel}) 370 (100, M⁺); ¹H NMR (C₆D₆) δ 7.90 (m, 2 H_o), 7.40 (m, 2 H_m + H_p), 4.06 (s, Cp), borole 5.35 (s, 3-/4-H), (CH₂)₂CHCH₂ 1.75 (dd, ²J_{AB} = 15.5 Hz, ³J_{A2} = 6.8 Hz, 1-H_A), 1.50 (dd, ²J_{AB} = 15.5 Hz, ³J_{B2} = 6.8 Hz, 1-H_B), and -0.3 to +0.5 (m, (CH₂)₂CH), -6.1 (s br (11 Hz), FeH); ¹¹B NMR (C₆D₆) δ -7.1; ¹³C NMR (C₆D₆) δ 135.6 (d, ¹J = 155 Hz, 2 C_o), 125.8 (C_p), signal of C_m hidden, 74.6 (d, ¹J = 178 Hz, C_p), borole 93.5 (s br (70 Hz), C-2/-5) and 87.6 (d, ¹J = 164 Hz, C-3/-4), (CH₂)₂CHCH₂ 36.5 (t, ¹J = 125 Hz, 2 C-1), 11.6 (d, ¹J = 160 Hz, 2 C-2), 5.0 (t, ¹J = 160 Hz, 2 C-3), and 4.5 (t, ¹J = 161 Hz, C-3').

Reaction of 1a with 1 Equiv of CNBu^t. NMR Experiment. CNBu^t (97 μL, 0.86 mmol) was added to **1a** (0.209 g, 0.80 mmol) in 2 mL of C₆D₆. The solution was kept at room temperature for 18 h while the reaction was monitored by NMR spectroscopy; the four compounds **1a** (29% of total of iron complexes), **9a** (53%), **11a** (18%), and free cyclopentadiene (amount approximately equivalent to **11a**) that were observed.

9a: ¹H NMR (C₆D₆) δ 7.52 (m, 2 H_o), 7.22 (m, 2 H_m + H_p), 3.98 (s, Cp), C₄H₅B 5.98 ("t", ³J₃₄ = ³J₂₃ = 4.1 Hz, 3-H), 4.53 (dd, ³J₂₃

= 4.1, ⁴J₂₄ = 1.9 Hz, 2-H), 4.00 (m, partly hidden by Cp signal), 4-H), 1.60 (d, ²J_{5endo,5exo} = 15.7 Hz, 5endo-H), and 1.31 (d, ²J_{5exo,5endo} = 15.7 Hz, 5exo-H), 0.93 (s, Bu^t); ¹¹B NMR (C₆D₆) δ 35.8; ¹³C NMR (C₆D₆) δ 178.7 (s, CN), 135.3 (d, ¹J = 155 Hz, 2 C_o), signals of C_m and C_p hidden, 76.5 (d, ¹J = 176 Hz, Cp), C₄H₅B 92.1 (d, ¹J = 164 Hz, C-3), 59.9 (d, ¹J = 162 Hz, C-4), and C-2 and C-5 not observed, 56.1 (s, CMe₃), 30.5 (q, ¹J = 128 Hz, CMe₃).

Preparation of 11a. CNBu^t (0.22 mL, 1.93 mmol) was added to a solution of **1a** (0.480 g, 1.84 mmol) in Et₂O at 0 °C. After the reaction mixture was stirred for 15 h at room temperature, the volatiles were removed in vacuo. Chromatography of the residue on alumina (20-cm column) with hexane/Et₂O (8/1) gave a red band of **1a** (0.23 g, 50%) and a yellow band of **11a** (0.134 g, 17%).

11a: red, air-stable crystals; mp 88 °C; dec pt >220 °C; MS *m/z* (*I*_{rel}) 445 (80, M⁺), 362 (96, M⁺ - CNBu^t), 306 (82, 362 - C₄H₆), 279 (82, M⁺ - 2 CNBu^t), 250 (67, 362 - 2 C₄H₆), 223 (100, 279 - C₄H₆), 196 (82, M⁺ - 3 CNBu^t); IR (Et₂O, cm⁻¹) 2126 s (CN), 2046 vs; ¹H NMR (CD₃COCD₃) δ 7.61-7.48 (m, 2 H_o), 7.22-7.07 (m, 2 H_m + H_p), borole 4.58 (m, ³J + ⁴J = 5.9 Hz, 3-/4-H) and 2.83 (m, ³J + ⁴J = 5.9 Hz, 2-/5-H), 1.27 (s, 3 Bu^t); ¹¹B NMR (CD₃COCD₃) δ 15.7; ¹³C NMR (CD₃COCD₃) δ 179.2 (s, 3 CN), 135.2 (d, ¹J = 154 Hz, 2 C_o), 127.6 (d, ¹J = 155 Hz, 2 C_m), 126.2 (d, ¹J = 158 Hz, C_p), borole 88.1 (d, ¹J = 165 Hz, C-3/-4) and 68.7 (d br, ¹J = 158 Hz, C-2/-5), 56.9 (s, 3 CMe₃), 31.5 (q, ¹J = 128 Hz, 3 CMe₃). Anal. Calcd for C₂₅H₃₆N₃BF₂: C, 67.44; H, 8.15; N, 9.43. Found: C, 67.56; H, 8.12; N, 9.57.

Reaction of 1a-*d*₃ with CNBu^t. The NMR experiment described above for **1a** was repeated with **1a-*d*₃**. Isotopic purity of the complex products was estimated from intensities of residual proton signals.

9a-*d*₃: ¹H NMR (80 MHz, C₆D₆) C₄H₅B δ 6.01 (d, 4-H) and 4.03 (d, 3-H) as AB system with ³J₃₄ = 3.6 Hz, only residual intensity for signals at 4.53 (5-H), 1.60 (2endo-H) and 1.31 (2exo-H).

11a-*d*₃: ¹H NMR (80 MHz, C₆D₆) borole δ 5.07 (s, 3-/4-H), only residual intensity for 2-/5-H signal.

Reaction of 1a-*d*₃ with CNBu^t and Trapping of the Cyclopentadiene Formed. CNBu^t (1.0 mL, 8.8 mmol) was added to **1a-*d*₃** (1.19 g, 4.5 mmol) in 20 mL of toluene. After the mixture was stirred at room temperature for 6 h, the volatiles were condensed into a cold flask (cooled by liquid nitrogen), containing maleic acid anhydride (0.33 g, 3.4 mmol). Then the flask was heated to reflux temperature for 3 h. Removal of the volatiles in vacuo left a white residue, which was examined by mass spectroscopy. The isotopic pattern at *m/z* 165 indicated 85% monodeuteration for the adduct **12**.

Preparation of 10. A mixture of Fe(CO)₂(CNBu^t)(C₄H₄BPh)⁹ (0.900 g, 2.70 mmol) and cyclopentadiene (0.4 mL, 4 mmol) in 80 mL of hexane was irradiated at 0 °C to produce ca. 5 mmol of CO (200 min). The mixture was concentrated to 10 mL and cooled to -30 °C to give a brown powder (0.71 g) consisting of **13** (25%) and **10** (75%). Chromatography on alumina (20-cm column) with hexane at -30 °C yielded three bands, a yellow band of **13** (23%), a red band with **10** (25%), and a red band with **11a** (15%) resulting from decomposition of **10** on the column.

10: dec pt 90 °C; IR (toluene, cm⁻¹) 2112 s (CN), 2080 m; ¹H NMR (C₆D₆) δ 8.05 (m, 2 H_o), 7.38 (m, 2 H_m + H_p), borole 4.86 (m, 3-/4-H) and 2.77-2.64 (m, 2-/5-H and 1-/4-H of C₅H₆), C₅H₆ 5.74 (m, 2-/3-H), 2.14 (dm, ²J_{AB} = 12.3 Hz, 5-H_A) and 1.71 (dm, ²J_{AB} = 12.3 Hz, 5-H_B), 1.00 (s, Bu^t); ¹¹B NMR (C₆D₆) δ 17.8; ¹³C NMR (C₆D₆) δ 183.2 (s, CN), 135.4 (d, ¹J = 156 Hz, 2 C_o), signals of C_m and C_p hidden, borole 88.6 (d, ¹J = 164 Hz, C-3/-4) and 64.3 (d br, ¹J = 154 Hz, C-2/-5), C₅H₆ 79.7 (d, ¹J = 175 Hz, C-2/-3), 57.5 (d, ¹J = 167 Hz, C-1/-4), and 42.0 (t, ¹J = 126 Hz, C-5), 56.7 (s, CMe₃), 30.2 (q, ¹J = 125 Hz, CMe₃).

Reaction of 10 with Excess CNBu^t. CNBu^t (20 μL, 180 μmol) was added to a solution of **10** (20 μg, 58 μmol) in 0.5 mL of C₆D₆. An instantaneous change of color from red to light orange occurred. The NMR spectrum of the reaction mixture showed complete conversion of **10** to **11a** and free cyclopentadiene.

Table 9. Crystallographic Data, Data Collection Parameters, and Refinement Parameters

	1d	1f
formula	C ₁₉ H ₂₃ BFe	C ₁₈ H ₂₁ BFe
fw	318.05	304.02
space group	I4 ₁ /a (No. 88)	P2 ₁ /n (No. 14)
a, pm	2806.1(4)	1180.9(2)
b, pm		844.3(1)
c, pm	824.5(2)	1577.8(1)
β, deg		102.11(1)
V, nm ³	6.491(2)	1.538(4)
Z	16	4
density (calc), g cm ⁻³	1.301	1.313
cryst size, mm ³	0.12 × 0.10 × 0.06	0.33 × 0.29 × 0.10
μ(Mo Kα), cm ⁻¹ ^a	0.91	0.97
radiation (λ, pm)	Mo Kα (71.069)	Mo Kα (71.069)
monochromator	graphite	graphite
temp, K	120	125
scan mode (2θ range, deg)	ω-2θ (3-50)	ω-2θ (3-50)
no. of unique rflns	2754	2721
N _o , no. of obsd rflns ^b	2187	2554
N _p , no. of params refined	167	209
R ^c	0.047	0.037
R _w ^d	0.042 ^e	0.039 ^f
residual electron density, 10 ⁻⁶ e pm ⁻³	0.51	0.54

^a No corrections for absorption and extinction were applied. ^b $F_o \geq 4\sigma(F)$. ^c $R = \sum ||F_o| - |F_c|| / \sum |F_o|$. ^d $R_w = [\sum w(|F_o| - |F_c|)^2 / \sum w|F_o|^2]^{1/2}$. ^e $w^{-1} = \sigma^2(F_o) + 0.000137F_o^2$. ^f $w^{-1} = \sigma^2(F_o) + 0.001F_o^2$.

Reaction of 1c with Excess CNBu^t. NMR Experiment. CNBu^t (40 μL, 360 μmol) was added to a solution of 1c (35 mg, 120 μmol) in 0.5 mL of C₆D₆. The solution was kept at room temperature for 30 days; the reaction was monitored by NMR spectroscopy, finally giving 9c (25%), 11c (75%), and free cyclopentadiene (amount approximately equivalent to that of 11c).

9c: ¹H NMR (C₆D₆) δ 7.89 (m, 2 H_o), 7.39 (m, 2 H_m + H_p), 3.81 (s, Cp), C₄H₅B 5.07 (d, 3-H) and 4.81 (d, 4-H) as AB system with ³J₃₄ = 3.9 Hz, 2.16 (s, 2-Me), 1.83 (s, 5-Me), and 1.35 (s, 5-H), 0.88 (s, Bu^t).

11c: ¹H NMR (C₆D₆) δ 8.18-8.06 (m, 2 H_o), 7.55-7.23 (m, 2 H_m + H_p), borole 4.68 (s, 3-/4-H) and 2.00 (s, 2-/5-Me), 1.04 (s, Bu^t).

Crystal Structure Analysis of 1d and 1f. Suitable crystals of 1d and 1f were obtained from concentrated hexane solutions at low temperatures (-78 °C). Pertinent crystallographic data are collected in Table 9.

Electrochemical Procedures. Cyclic voltammograms were measured using a Princeton Applied Research (PAR), EG&G) Model 173 potentiostat and Model 175 function generator, a

Metrohm electrochemical cell, and Metrohm platinum-disk electrodes. Moderate sweep rate cyclic voltammograms were recorded on a Houston Instrument Series 2000 X-Y recorder, and rapid scan rate data were obtained on a Hameg HM 208 two-channel storage oscilloscope. All potentials are given in V vs a SCE as reference electrode that was equipped with a salt bridge (Metrohm) of composition identical with that of the investigated solution. Ferrocene was used for calibration and as an internal standard. Purification of electrolytes and solvents and cell measurements were conducted under argon. Bu₄NPF₆ (Fluka electrochemical reagent grade) was dried at 110 °C for 20 h in vacuo before use. DME (Aldrich 99+ %) was passed through a column of activated basic alumina (ICN Alumina B Super I, activated at 280 °C for 2 days in vacuo) and distilled twice before use. The solvent was stored under argon, and freshly prepared solutions of electrolytes were stored in Schlenk tubes equipped with Teflon valves.

EPR and Paramagnetic NMR Measurements. Pure solutions of [Li(TMEDA)]5a⁹ in THF-d₃ allow the observation of diamagnetic NMR spectra ($f_p = 0$). Stepwise oxidation was performed in the NMR tube by briefly exposing the solution to air and subsequent strong shaking. This procedure yields 5a/5a⁻ mixtures with increasing contents of 5a. For complete oxidation ($f_p = 1$) an excess of oxygen and strong shaking is required. This sample was also used for the EPR measurement after cooling to 100 K. To prove the chemical reversibility of the oxidation, a second sample of partly oxidized [Li(TMEDA)]5a was prepared in THF-d₃. The sample tube was fitted with a potassium mirror at the top and sealed. Reduction was performed by turning the tube upside down several times. Again a series of NMR spectra are obtained which fit perfectly to the data of the oxidation experiment. This method has been employed previously in the ¹H NMR characterization of paramagnetic multidecker sandwich and metallacarborane complexes.²⁴ The paramagnetic mole fractions f_p are determined via the linearity of δ_{obs} (Figure 9).

Acknowledgment. We thank the Deutsche Forschungsgemeinschaft and the Fonds der Chemischen Industrie for generous support of this work and an FCI graduate fellowship for T.C.

Supplementary Material Available: Tables of crystal data and structure solution and refinement details, bond distances and angles, anisotropic thermal parameters, and hydrogen atom coordinates for 1d and 1f (14 pages). Ordering information is given on any current masthead page.

OM930511C